Acta of Bioengineering and Biomechanics
Vol. 18, No. 4, 2016

Original paper
DOI: 10.5277/ABB-00563-2016-03

Comparative study of potential whiplash injuries for different occupant seated positions during rear end accidents

SENAD OMEROVIĆ[1]*, ERNST TOMASCH[2], ANDREAS J. GUTSCHE[2], IVAN PREBIL[1]

[1] Mechanical Faculty, University of Ljubljana.
[2] Vehicle Safety Institute, Graz University of Technology.

Purpose: Whiplash injuries to the cervical spine represent a considerable economic burden on society with medical conditions, in some cases persisting for more than a year. Numerous studies of whiplash injuries have been made for occupant normal seated position, leaving the analysis of neck injuries for out-of-normal positions not well documented. For that purpose, a detailed human cervical spine finite element model was developed. *Methods:* The analysis was made for four most common occupant seated positions, such as: Normal Position with the torso against the seat back and the head looking straight ahead, Torso Lean forward position with the torso away from the seat back for approximately 10°, Head Flexed position with the head flexed forward approximately 20° from the normal position and Head-Flexed with Torso Lean forward position with the head flexed forward approximately 20° and torso 10° from the normal position. *Results:* The comparative study included the analysis of capsular ligament deformation and the level of S-curvature of the cervical spine. The model developed predicted that Head Flexed seated position and Head-Flexed with Torso Lean forward seated position are most threatening for upper and lower cervical spine capsular ligament, respectively. As for the level of S-curvature, the model predicted that Head-Flexed with Torso Lean forward seated position would be most prone to neck injuries associated with it. *Conclusions:* This study demonstrated that the occupant seated position has a significant influence on potential whiplash injuries.

Key words: *biomechanics, whiplash, LS-Dyna*

1. Introduction

Human neck presents a complex anatomical structure comprising of hard tissues (cervical vertebrates from C1 to C7) and soft tissues (ligaments, cartilages, intervertebral discs (IVDs), muscles, nerves, the spinal cord, etc.). During low speed rear end traffic accidents, these soft tissues are usually subjected to the loads and movements above their physiological range, causing them to be injured. These injuries, also known as whiplash associated disorders (WAD), are the most common type of injuries sustained in a traffic accident and can range from chronic neck pain to fatal hard tissue fracture according to Québec Task Force (QTF) grades of WAD [20].

The studies have shown that associated cost of cervical spine injuries are estimated 10 billion Euros per year in the European Union [8]. This represents the significant burden on society with injury symptoms, in many cases persisting for more than a year.

Low severity injuries are more frequent than traumatic injuries. They are often attributed to muscle strain, ligament sprain, intervertebral disc injury and neural injury.

Muscle strain happens when the muscle is stretched during the impact. Numerous factors, such as the level of muscle activation and muscle kinematic (lengthening or shortening) prior to the impact, which are difficult to be determined, make the prediction of the muscle injury during the traffic accidents a major issue.

* Corresponding author: Senad Omerović, Mechanical Faculty, University of Ljubljana, Aškerčeva 6, 1000 Ljubljana, Slovenia. Tel: +38640181669, e-mail: senad.omerovic@fs.uni-lj.si
Received: January 20th, 2016
Accepted for publication: March 18th, 2016

Ligament injuries occur when they are stretched above their psychological range of motion. A typical ligament (Force/Elongation) response includes a toe region, linear and failure region depicted in Fig. 1 [25]. Toe region corresponds to the ligament initial stretching during which collagen fibres are not aligned. As the stretching continues, collagen fibres gradually align making the (Force/Elongation) ligament response linear. Larger deformations in this region can cause initial micro failure leading to pain. Beyond the linear region, individual collagen fibres began to tear, leading to reduction in ligament stiffness, which can lead to serious pain and joint instability.

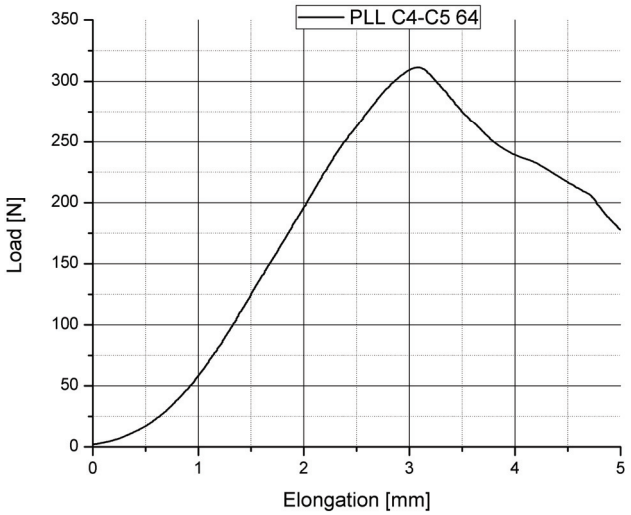

Fig. 1. Posterior longitudinal ligament (ALL) response [25]

The IVD can also be injured in traffic accidents. They are comprised of: outer fibrous ring, made of several layers of fibro cartilage called annulus fibrosis and centrally situated gelatine such as structure nucleus pulposus. The upper and lower surfaces of vertebral body are flattened and rough in order to give attachment to the intervertebral discs. These surfaces are vertebral endplates which are in direct contact with the intervertebral discs forming the joint. During the impact, especially the lower cervical spine experiences complex loading which consists of extension and posteriors shearing and compressive force, causing the disc herniation and cartilaginous endplate injuries during the whiplash [15].

Neural injuries can occur in dorsal root ganglia during the whiplash. They are associated with the increased pressure of blood and cerebrospinal fluid in the spinal canal, causing the spinal ganglion nerve cell body membrane dysfunctions, which can lead to neck pain, cervicogenic headache, vertigo, vision disturbance and neurological symptoms in the upper extremities [19].

All of the above mentioned injuries present a variety of conditions that are commonly known as whiplash associated disorders (WAD) [20]. WADs are generally graded in to five different categories described in Table 1.

Table 1. WAD classification [20]

WAD Grade	WAD clinical description
0	No complaint about the neck. No physical signs.
I	Neck complaint of pain, stiffness or tenderness only. / No physical sign(s).
II	Neck complaint AND musculoskeletal sign(s). / Musculoskeletal signs include decreased range of motion and point tenderness.
III	Neck complaint AND neurological sign(s). / Neurological signs include decreased or absent deep tendon reflexes, weakness and sensory deficits.
IV	Neck complaint AND fracture or dislocation.

Several anatomical sites in the neck have been postulated for a whiplash injury, including the facet joints capsular ligament (CL), spinal ligaments, intervertebral discs, vertebral arteries, dorsal root ganglia and neck muscles [19].

Facet joints injury represents the most common source of pain in whiplash injuries [1]. For each pair of cervical vertebra from C2 to C7, there are two facets joints comprising of synovial joint enclosed in a ligament, known as the facet capsule. Two mechanisms of facet joint injury have been documented: pinching of the synovial fold and excessive strain. The pinching mechanism was defined by abnormal rotation of cervical vertebra about a higher instantaneous center during the whiplash exposure comparing to the normal voluntary motion. This rotation of cervical vertebra compresses the posterior facet joints, pinching the synovial fold [9]. Excessive strain of 29 to 40 percent of facet joints during the whiplash exposure has been documented [19] while sub-catastrophic and catastrophic failures are 44 ± 12% and 103.6 ± 80.9%, respectively [18]. A normal voluntary neck flexion produces strain of only 6 ± 5 percent [16].

Occupant neck kinematic during the rear end traffic accidents can be divided into 3 stages. The first stage (S-curve phase) includes loading on the torso and shoulders through the back of the seat, while the head remains stationary. The forward motion of the torso and shoulders relatively to the stationary head results in head lag, while the neck takes the shape of the S-curve. This phase is also documented as hypertranslation of the head.

In the second phase, the cervical spine and the head are in extension, forming the C-shape curve in sagittal plane. The neck kinematic described stretches the facet joint capsular ligament with the frequent outcome of acute neck instability [17].

The hydrodynamic injury mechanism occurs in the first phase (S-curve) of cervical spine kinematic, with extension and flexion, occurring concurrently in lower and upper portion of the neck, respectively. This may lead to protrusion or inward buckling of the ligament flavum (LF), compromising the neural space. Further, the decreased canal volume results in increased hydrodynamic pressure and increased outward flow of its contents. Increased blood and cerebrospinal fluid pressure damage the nerve root, causing the head and neck pain [13], [30].

Based on different aspects of the aforementioned studies, it can be concluded that whiplash injury covers a wide range of medical conditions and symptoms with a various injury mechanism causing them. Additionally, the variations of occupant positions during the impact further contribute to significant variability of whiplash epidemiological data [2].

The understanding of WAD requires detailed knowledge on the cervical spine dynamics and the process of injury occurrence in soft and hard tissues.

The human neck injury tolerances to the inertial loads have been investigated intensively for many years. At first, the obtained information was used for military purposes, with later inclusion for increasing the automotive safety. Numerous studies have been made with: cadavers, anthropometric test device (ATD), volunteers and computer modelling with a great majority of them being for occupant normal seated positions, leaving the analysis of neck injuries for out-of-normal positions not well documented [11], [21].

The purpose of the present study was to compare the loads on the proposed sources of the neck pain associated with whiplash injuries for most common occupant seated positions depicted in Fig. 2. Investigated seated positions in this study are:

Normal position (NP.), with the occupant's head looking straight forward and the torso against the seat back.

Torso Lean position (TL), with the torso angle of approximately 10 degrees from the normal position.

Head Flex position (HF), with the torso in the normal position and the head flexed forward approximately 20 degrees from the normal position.

Head Flex / Torso Lean position (HF/TL), with the subject's head flexed forward approximately 20 degrees and with the subject's torso leaned forward approximately 10 degrees [11].

A comparative analysis was made with a developed FE model of cervical spine for medium severity rear end impact according to the Euro NCAP whiplash testing procedures [12]. FE model included passive musculature, detailed intervertebral discs with nucleus and annulus models, non-linear tension only ligaments, cartilages and facet joints as soft tissues. Skull, cervical vertebras and torso were modelled as rigid bodies. The FE model developed also included a detailed atlas axial occipital joint with the apical, alar, tectorial membrane and transverse ligaments (Fig. 3).

The model developed, as demonstrated in this study was able to predict how different occupant seated positions could influence the kinematic and the loads on individual anatomical structures. The comparative study included the analysis of strain for CL, anterior longitudinal ligament (ALL), PLL, LF and the level of S-curvature of the neck.

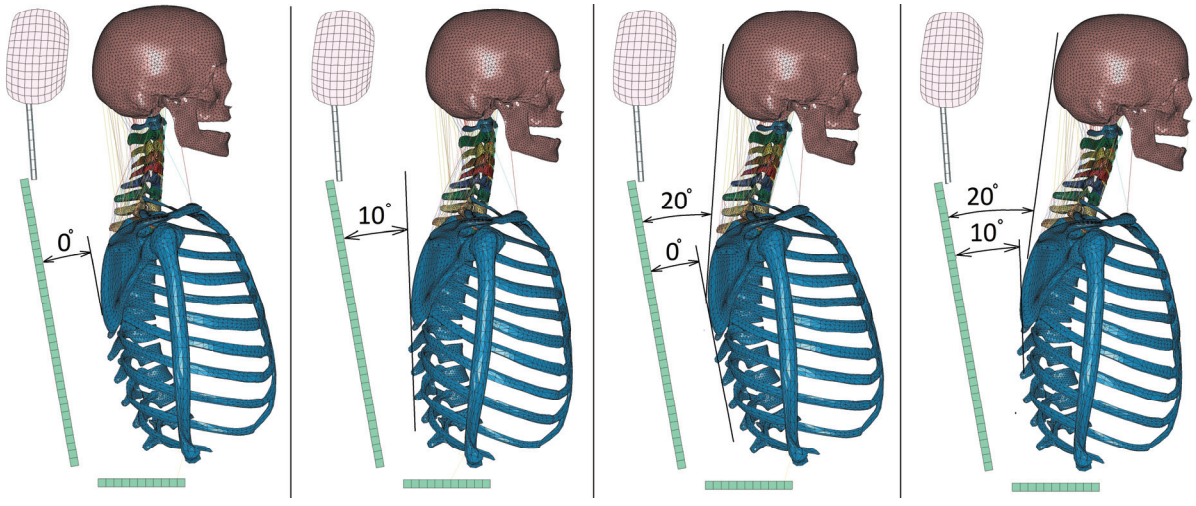

Fig. 2. Four seated positions investigated: NP, TL, HF and HF/TL

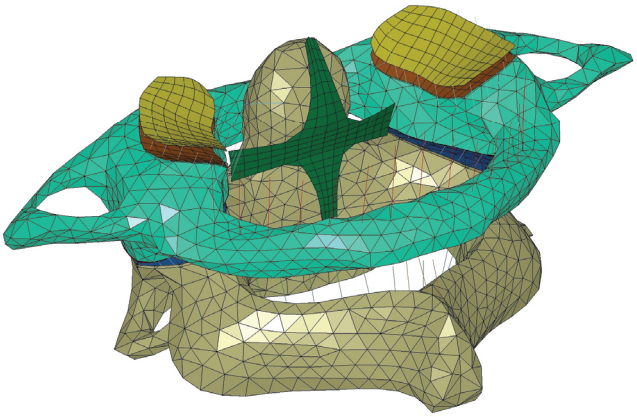

Fig. 3. C1-C2 joint

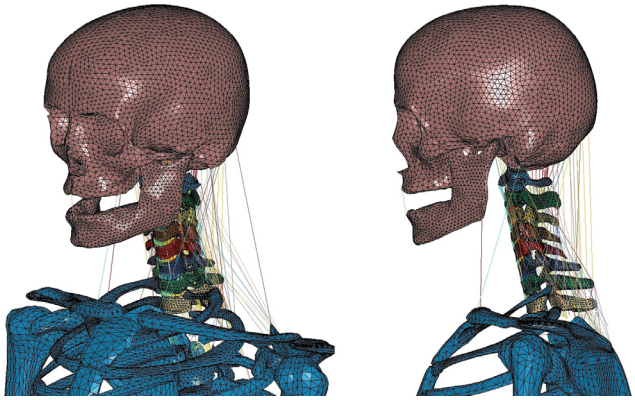

Fig. 4. Developed FEM

2. Materials and methods

The FE model of the cervical spine was based on the precise geometrical models of individual anatomical structures, with a focus on their mechanical properties. The FE model developed included seven cervical vertebras, skull, torso, IVD, cervical ligaments, facet joints, cartilages and neck muscles. The whole FE model was generated by using LS PrePost 4.2 (Livermore Software Technology Corporation), while the simulations were enabled by a solver for explicit analyses using the Central Difference method. The model was described with a series of nonlinear ordinary differential equations. Solver used for solving them was LS-Dyna Version R7.1.1.

The model as a whole had three degrees of freedom, two translations in sagittal plane and one rotation along axis normal to sagittal plane. Acceleration for torso and first thoracic vertebra (T1) was defined in anterior direction (X-axis) using the BOUNDARY_PRESCRIBED_MOTION_RIGID card in LS-Dyna with additionally defining the angular rotation of T1. Actual modelling of the contact between the torso and the seat that can accurately describe the compression of chest and the seat during the rear end impact demands the precise FE model of both. This is far beyond the scope of this research. Therefore, in order to precisely transfer the impact pulse to the neck we prescribed the acceleration to the head rest, thoracic vertebra T1 and torso according to the measured data using the above mentioned card in LS-Dyna. Head rest acceleration was modelled to be equal to those of the sled while using the material model BLATZ-KO_FOAM and Shear modulus of 0.1 MPa to describe its material properties.

Figure 4 shows the newly developed FEM model which included 235,975 finite elements, with the simulation time step of 711 ns. The coordinate axes of the geometrical model were oriented so that the X-axis lies in the anterior direction, Y-axis in the lateral direction and Z-axis in the inferior direction.

Model geometry and material properties

Skeleton geometry (Fig. 5), used for meshing, was developed by Zygote Media Group from computer tomography scans of the 50th percentile male and was carefully modelled to retain subtle anatomical nuances unique to specific bones. Soft tissues such as ligaments, cartilages and intervertebral discs were incorporated according to their anatomical location.

Also, in the model there are sixteen neck muscle pairs included: longus colli, scalenus anterior, longus capitis, scalenus medius, lumped hyoid, scalenus posterior, trapezius, sternocleidomastoid, splenius capitis, splenius cervicis, semispinalis capitis, semispinalis cervicis, longissimus capitis, longissimus cervicis, levator scapulae, multifidus cervicis.

Biological soft tissues generally have non-linear, viscoelastic and orthotropic mechanical properties. In the FE model developed, the ligaments were modelled using 1D non-linear spring with damping. Typically, ten beam elements were used to model each ligament. Cartilages were modelled on each articular surface with 2D shell elements with viscoelastic material model. The average thickness was around 1 mm depending on the gaps of sliding surfaces. Nucleus pulposus and annulus fibrosus of IVD were modelled using solid hexahedral elements with viscoelastic and elastic material models, respectively. The muscles were modelled with 1D non-linear passive beam element. This is mainly because most occupants do not expect rear end accidents to happen. Additionally, the FE model developed was validated with the rear end

impact results gained from Post Mortem Human Specimen (PMHS) sled tests and not volunteers.

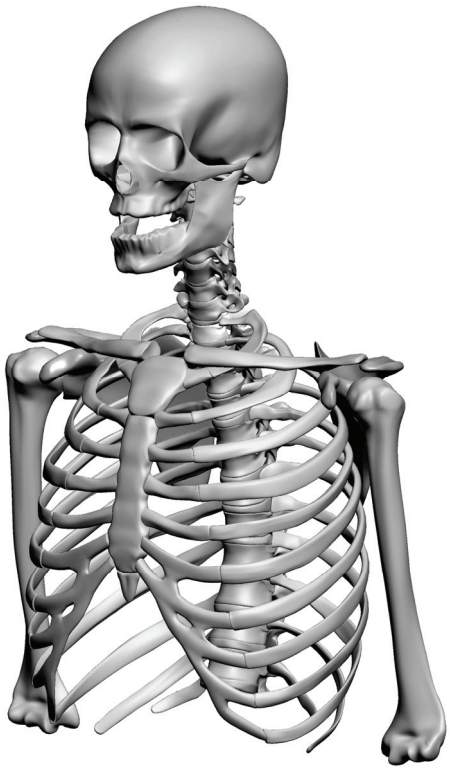

Fig. 5. Solid geometrical 3D model of human skeleton by Zygote Media Group

Cervical vertebras were modelled with 3D tetrahedral elements for cancellous bone and 2D shell elements for a cortical bone with the thickness of 0.55 mm. Since the deformations of bones during the low speed rear end accidents are notably smaller than those of soft tissue, they were modelled as rigid bodies to reduce the computation time. The skull was also modelled as a rigid body with mass and inertial properties defined by ELEMENT_INERTIA at the head center of gravity. The material properties for soft and hard tissues are defined in Table 2.

FE model validation

The cervical spine model developed was validated against the data published in Kang [10] and a series of PMHS pneumatic sled tests performed for investigated medium EuroNCAP rear end impact. Re-use of PMHS for impact tests is acceptable if there are no any injuries sustained by PMHS during the previous tests. This is usually achievable in low severity and in some cases medium severity impact tests. Since we used medium severity impact for validation we opted to also include PMHS single impact test performed by Kang [10].

Kang's impact test results describe the head and cervical vertebras kinematics of PMHS during the rear end impacts, ranging from 8 to 11 g. Kinematics of

Table 2. Material properties

Cervical tissue	Finite element	Material model	Density	Material properties	Reference
Bones					
Cancellous	solid 3D	Rigid	1.1 g/cm^3	100 MPa	[3]
Cortical	2D shell	Rigid	2.0 g/cm^3	10000 MPa	[3]
Skull for PMHS2 and PMHS3	2D shell	Rigid		m =3.561 kg, I_{yy} =1.71e^4 kg mm^2	[26], [29]
Cartilage	2D shell	Viscoelastic	1.06 g/cm^3	K = 2.0 GPa, G_0 = 2.228 MPa, G_{inf} = 0.210 MPa, β = 0.248 s^{-1}	
Ligaments		Non linear elastic	1.2 g/cm^3		
ALL	1D beam			E = 30.28 Mpa	[24]
PLL	1D beam			E = 27.46 MPa	[24]
LF	1D beam			E = 5.46 MPa	[24]
CL	1D beam			E = 5 MPa	[28]
ISL	1D beam			E = 4.9 MPa	[28]
NL	1D beam			E = 4.9 MPa	[28]
Apical	1D beam			E = 20 MPa	[14]
Transverse ligament	Shell			E = 20 MPa	[14]
Alar	1D beam			E = 5 MPa	[23]
Anterior membrane	1D beam			E = 20 MPa	[23]
Posterior membrane	1D beam			E = 20 MPa	[23]
Annulus fibrosis	Solid	Elastic	1.2 g/cm^3	E = 3.4 MPa	[27]
Nucleus pulposus	Solid	Viscoelastic	1.36 g/cm^3	K = 2200 MPa, G_0 = 2 MPa, G_{inf} = 1.4 MPa, β = 1 s^{-1}	[27]
Muscles	1D beam	Passive			[7]

K: bulk modulus; G_0: short-term shear modulus; G_{inf}: long-term shear modulus; β: decay constant.

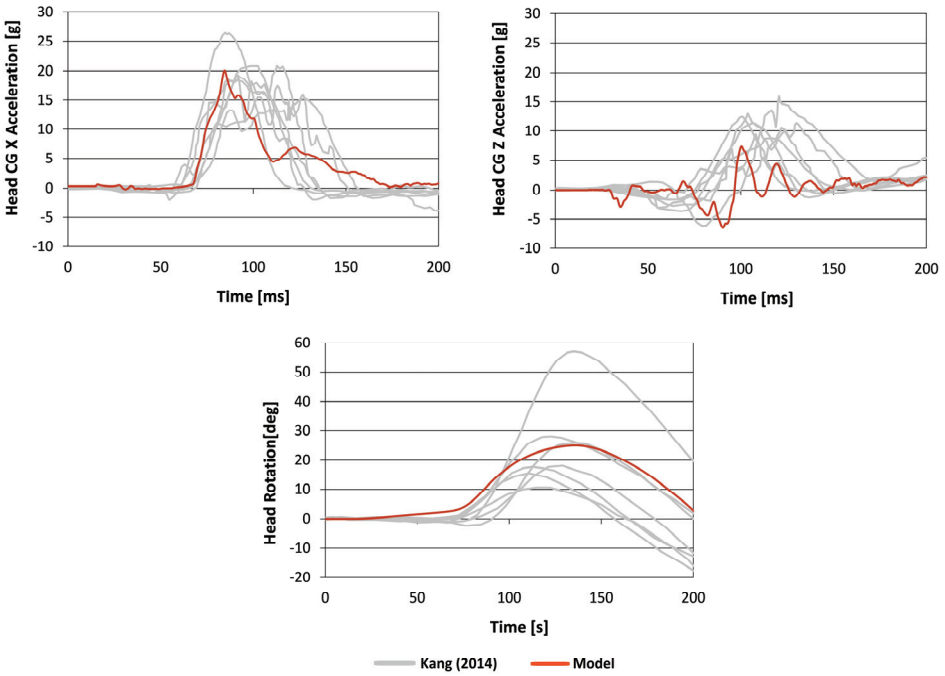

Fig. 6. Global kinematic head response

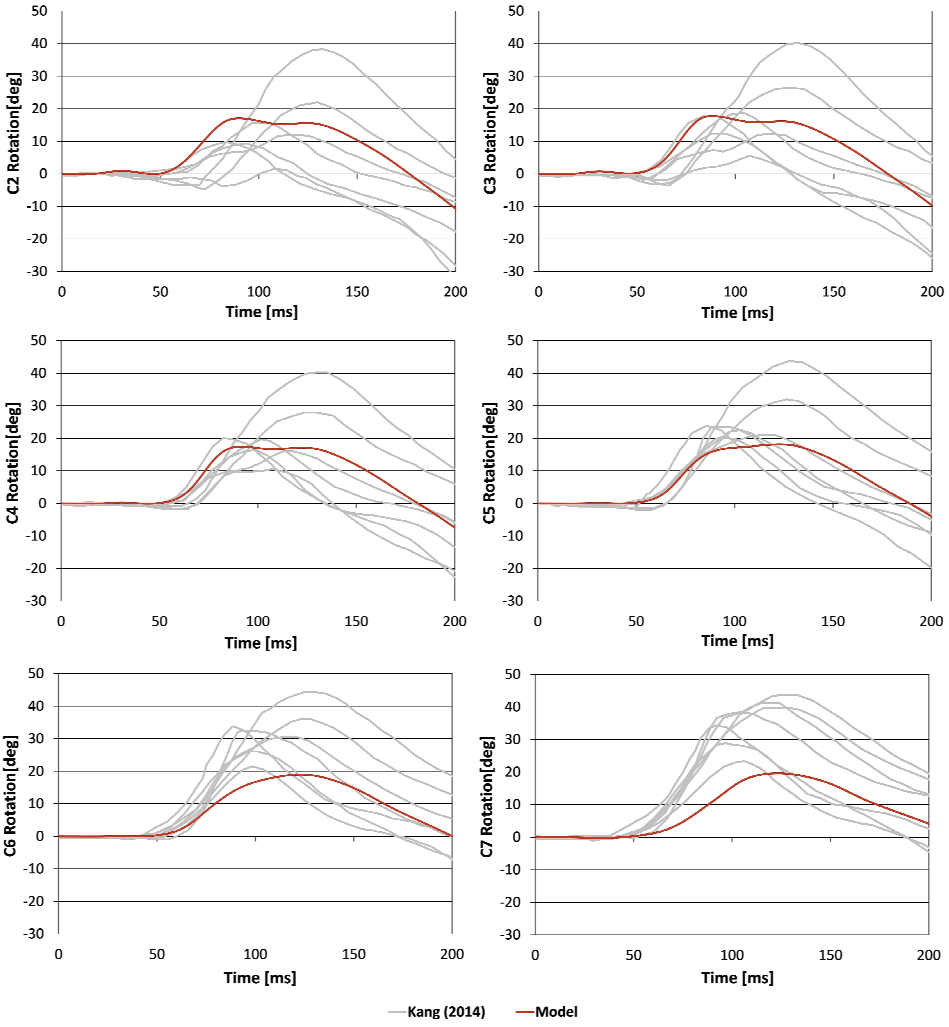

Fig. 7. Cervical vertebras kinematic

thoracic vertebra (T1), *x*-, *z*-acceleration and *y*-rotation, were also included in the published results and were used for defining the boundary conditions in the developed model. Tests were performed on HYGE sled test for three different pulses according to FMVSS 202a, JNCAP and 10.5 g at 24 km/h. A total of seven tests were conducted with seven different PMHS.

PMHS sled tests results that were performed by Kang [10] are depicted in Figs. 6 and Fig. 7. The model developed correlated well with the experimental results regarding the measured trajectories of the head and neck body segments and head accelerations.

In addition to that, we performed a series of PMHS pneumatic sled tests for the investigated medium severity rear end impact (Fig. 8) according to Euro NCAP testing procedure.

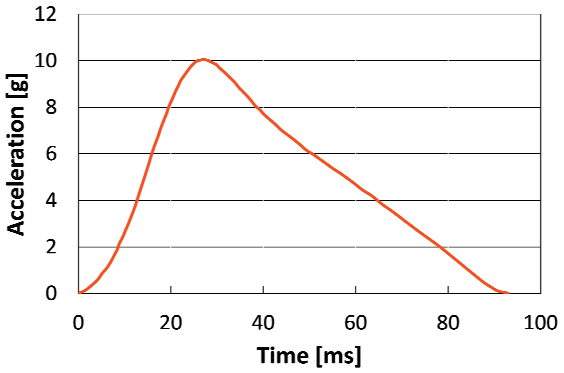

Fig. 8. Medium severity rear end impact, Euro NCAP whiplash testing

Four PMHS were tested on a pneumatic sled test device depicted in (Fig. 9).

At the time of the testing we had four PMHS at our disposal (three females and one male) through the University of Ljubljana, Faculty of Medicine, Body Donor Program. All of the PMHS had X-ray check and none of them have shown severely degenerated intervertebral discs, osteophytes or any previously documented spinal injury. PMHS variations are normal part of any PMHS test series since it is practically impossible to have PMHS of same sex, age and anthropometric data. For each PMHS two rear end impact tests were performed out of which only four (two of PMHS_2 and two of PMHS_3) could be used for verification purposes of the developed cervical spine model due to the testing equipment issues.

Table 3. PMHS data

PMHS	1	2	3	4
General information				
Weight [kg]	83	67	60	83
Height [cm]	178	160	158	171
Birth year	1939	1938	1925	1916
Gender (sex)	m	f	f	f
Body circumference [cm]	------	------	------	-------
Thorax	115	85	88	107.5
Waist	99.5	93	75	101
Hip	103.5	99.5	97.5	102
Head/neck dimensions [cm]	------	------	------	-------
Head circumference (1)	57	54	56	55
Neck circumference (3)	43	33	36.5	44
Head height (2a)	25	19	20	22
Head length (depth) (2b)	19	17	17	19
Head width (2c)	15.5	15	15.5	15.5
Chin head circumference (2)	69	63	67.5	68.5
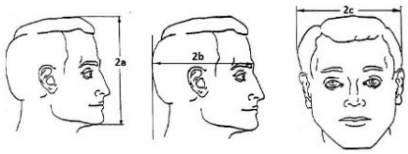				

Before the tests, the anthropometric measures were taken for each PMHS (Table 3). These measures were then used to scale the FE model developed, so it would geometrically correspond to PMHS. Since the

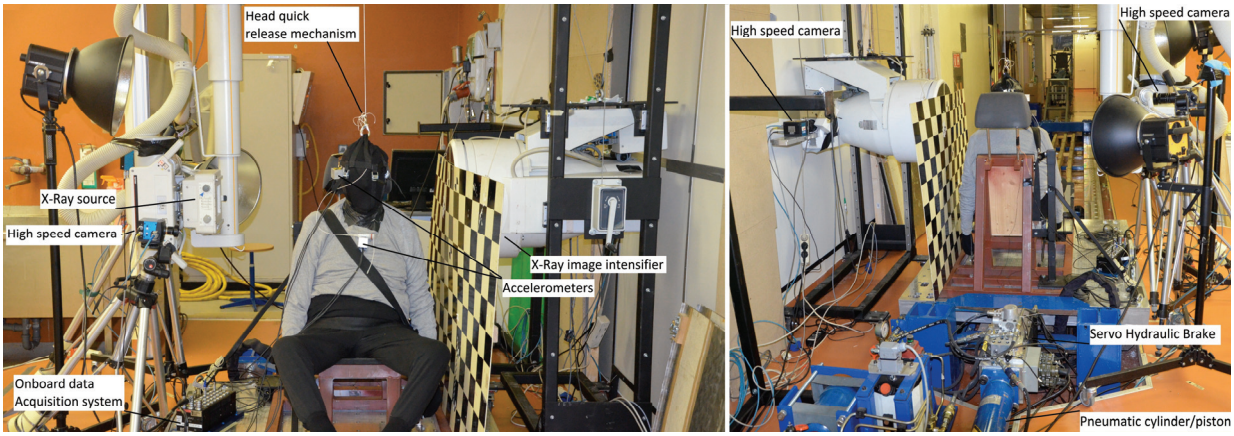

Fig. 9. PMHS on test sled device (front and rear view, respectively)

anthropometric data for PMHS_2 and PMHS_3 were very similar, one FE model was used to represent both PMHS_2 and PMHS_3. The head mass of PMHS was assessed from the PMHS height, posture and weight using the published data [26], [29]. The head inertia was calculated from the following equation

$$I_{yy} = 47.895 \cdot m\,.$$

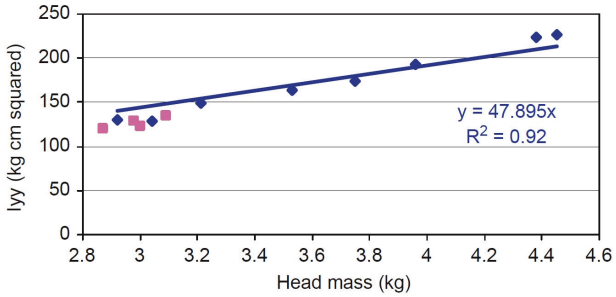

Fig. 10. Head lateral moment of inertia from literature [29]. Pink data points correspond to female specimens, and blue data points and the regression line correspond to male specimens

For each impact test, the initial positions of the PMHS's head and cervical vertebras were determined using the X-ray pictures (Figs. 11–14). This was later used to bring the FE model developed into the same positions for verification purposes.

The impact tests were performed on the pneumatic sled system that uses an active online (closed loop) control of the acceleration pulse by applying the hydraulic brake on the pneumatic piston rod. Therefore, each prescribed pulse could be reproduced without any previous calibration tests. Only the weight of the moving mass must be defined. The test results were obtained from three accelerometers and three video cameras (one was X-ray). The first tri-axial DSD 200 accelerometer was mounted at the approximated position of the head centre of gravity on the left side of the PMHS. The accelerometer was attached by screws directly into the skull to deliver accurate acceleration measurements. The second tri-axial DSD 200 accelerometer was attached directly into the sternum. The third tri-axial DSD 200 accelerometer was attached by inserting two screws into the first thoracic vertebrae (T1). The anatomic position of T1 was located by a medical doctor. The initial positions and orientations of accelerometers were measured prior to each test. The data from sternum and T1 accelerometers were analysed and transformed using the video data from local to global coordinates. These data were used together with the measured sled acceleration as bound-

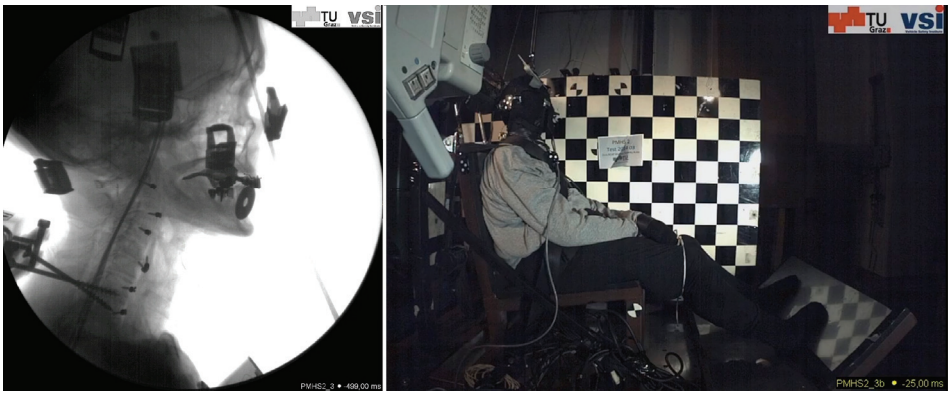

Fig. 11. PHMS_2 initial position for rear end impact no. 3

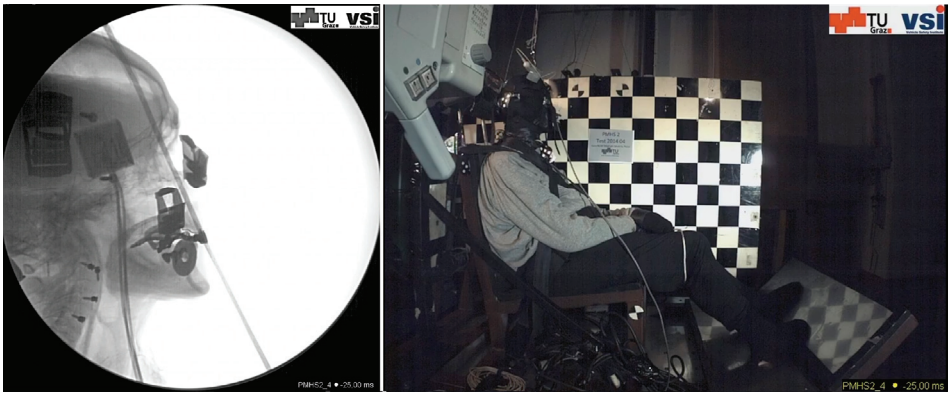

Fig. 12. PHMS_2 initial position for rear end impact no. 4

ary conditions for the developed cervical spine model while the measured head acceleration was used for model validation purposes.

Figure 15 depicts the test sled results for PMHS_2 impact no. 3 and 4 and PMHS_3 impact no. 1 and 2. Different seated positions in PMHS_2 and PMHS_3 resulted in different cervical spine curvature between them. PMHS_2 and PMHS_3 seated position was comparable to NP and HF/TL positions respectively. This also explains the higher head accelerations for PMHS_3, due to the more intense thoracic ramping for PMHS_3.

While for PMHS_2, the developed model predicted head acceleration results correlate well, for PMHS_3 the results proved to be more difficult to match. The difference was associated to the lack of damping in the model. This is caused by the absence of some soft tissues in the developed FE model such as skin, fat, digestive tract and airways. Additionally, by analysing the high speed X-ray videos, relative rotations of individual vertebras for all four PMHSs were determined. Results have shown that neck of PMHS_3 was stiffer than that of PMHS_2. This could

Fig. 13. PHMS_3 initial position for rear end impact no. 1

Fig. 14. PHMS_3 initial position for rear end impact no. 2

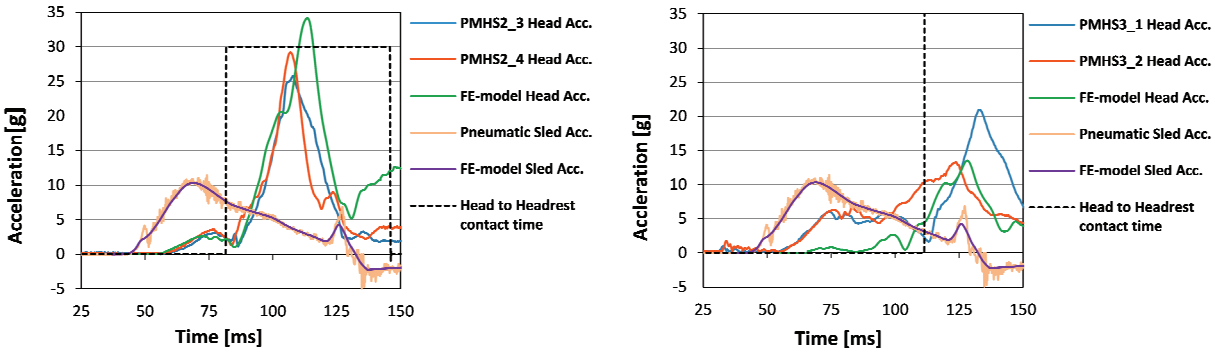

Fig. 15. Comparison of sled tests impact results and the developed model for PMHS_2 and PMHS_3, respectively

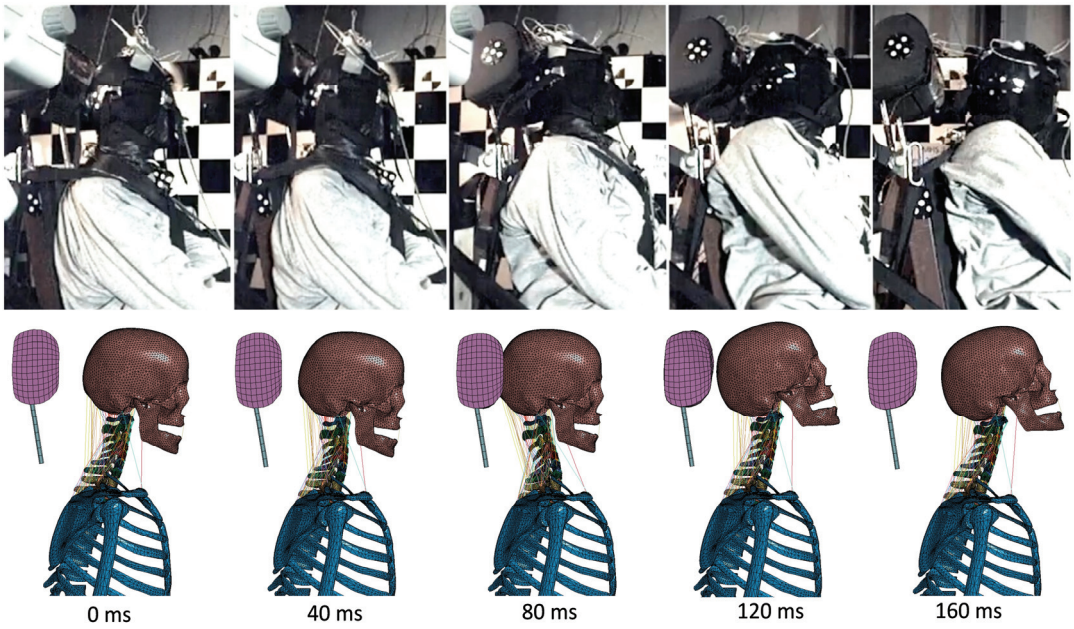

Fig. 16. Time-laps images of PMHS_2 and developed model head response

be explained with more degenerated and hence rigid IVDs in PMHS_3 than in PMHS_2.

Based on preformed validation process it can be concluded that the developed model was constructed accurately and was validated at a segmental level and at the whole cervical spine without calibration to any of the test conditions investigated. A comparison of PMHS_2 and developed model head response is depicted in Fig. 16.

3. Results

The comparative analysis of four different occupant seated positions included the analysis of peak ligament strains at a segmental level and the S-curvature of cervical vertebrae. The applied inertial load was according to the medium severity rear end impact, defined by Euro NCAP protocol [12]. The

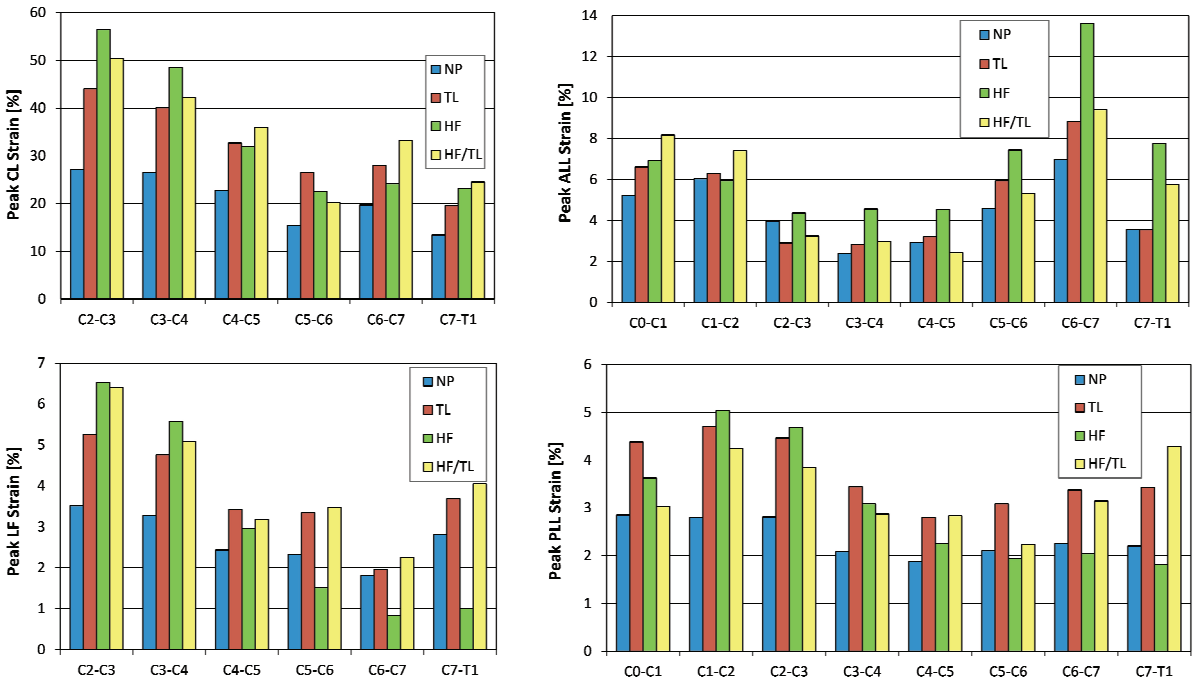

Fig. 17. Peak ligament strain predicted by the model for four seated positions under investigation

peak ligament strain was calculated as average maximal axial strain of discreet beam finite elements of each individual ligament (Fig. 17).

The model predicted the peak strain of 56.42% in CL for HF seated position in the upper portion of cervical vertebrae, while for lower part the predicted peak strain in CL was for HF/TL seated position. The same as for CL, the model predicted the peak LF strain of 6.53% to be in the upper portion of cervical vertebra for HF seated position and in the lower part the peak strain of 4.05% for HF/TL seated position. For ALL the model predicted peak strain of 8.17% in the upper portion of cervical vertebrae for HF/TL seated position and in the lower portion of cervical vertebrae peak strain of 13.63% for HF seated position. For PLL the model predicted the maximum strain of 5.03% for HF seated position in the upper portion of cervical vertebrae and in the lower portion the peak strain of 4.29% was predicted.

Beside the possible neck ligament injuries during the rear-end accidents there is also a possibility of damage to the nerve root in the spinal canal, causing the head and neck pain. This neural injury is caused by cervical spine kinematic with extension and flexion, occurring concurrently in the lower and upper portion of cervical vertebrae, forming the S-shape curve. Maximum S-curvature was defined as the time at which C2-C3 sustained maximum flexion [22]. The S-curvature of cervical vertebrae was quantified by measuring angles α and β between C2-C4 and C4-C7, respectively during the impact. The angles were calculated between the lower endplates of corresponding vertebras (Fig. 18). The predicted S-curvature for four seated positions investigated is depicted in Fig. 19.

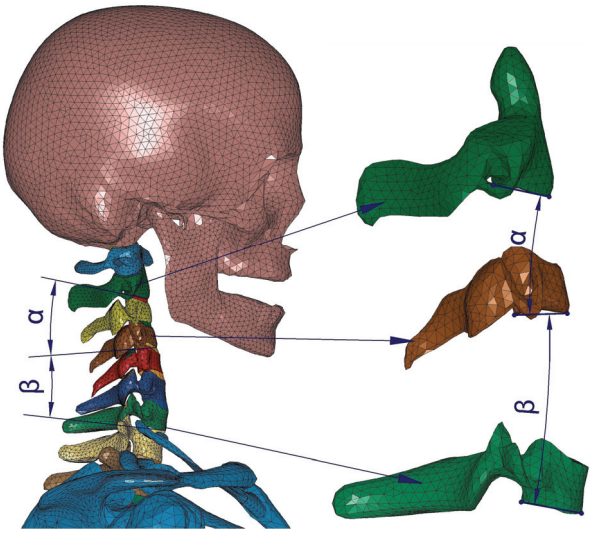

Fig. 18. Measurement of the level of S-curvature of cervical spine

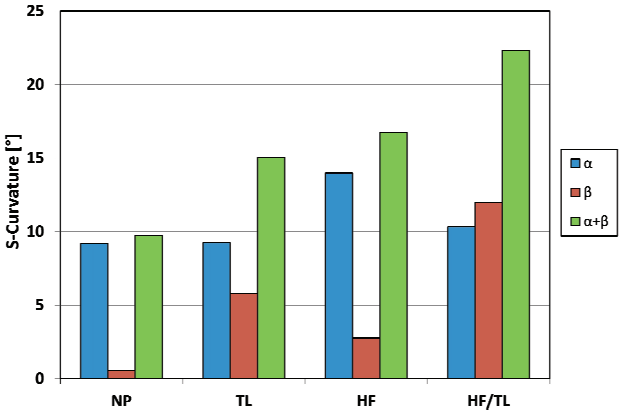

Fig. 19. Level of S-curvature of cervical vertebrae (model prediction)

4. Discussion

Capsular ligament injuries have been proposed as one of the main sources of neck pain for victims of rear end accidents with several studies supporting this theory [1], [9], [19]. A FE model of cervical spine was developed to assess the potential whiplash injury for different occupant seated positions. The results in this study are unique from previous one because they determined the strain of cervical ligaments such as CL, ALL, LF and PLL and describes how the maximum level of S-curvature of the neck is changed for various occupant seated positions. Additionally, this comparative analysis was performed for medium severity impact according to the EuroNCAP whiplash testing procedure which is also used in automotive industry for testing the seats and head restraints for increasing the whiplash protection.

The cervical spine FE model developed was based on the accurate 50th percentile male skeleton geometrical model. The material properties of soft tissues were used from the literature without any modification in the form of model calibration to any of the impact test data used for validation purposes. The model included passive musculature system which reflects sudden unanticipated rear end impact. Additionally, the model was validated with the sled test impact using PMHS and not volunteers.

Validations were made using two sets of data. The first set included the results published by Kang [10] for various rear end impact scenarios. The second set of data was obtained by performing a series of rear end impact tests using the PMHS on a pneumatic sled test device for medium severity impact according to the EuroNCAP whiplash test procedure. Since the model is not calibrated to particular experimental re-

sults this resulted in poor agreement with PMHS_3 impact results depicted in Fig. 15. This could be explained by the fact that the model developed was based on a healthy 50 percentile male skeleton geometry. Neither the IVD degeneration characteristic of older population nor the altered mechanical properties of soft tissues due to aging were considered.

For the rear end impacts under investigation, the FE model developed predicted the highest ligament strain of 56.42% for CL in the upper cervical spine during the HF-seated position, whereas for lower cervical spine, peak CL strain of 33.23% was measured. The published sub-catastrophic failure strain ranged from 35 ± 21% to 65 ± 74% [4], indicating a high risk that peak CL strains are within a sub-catastrophic failure. This corresponds to the biomechanical and clinical findings that the injury to the CL is a potential source of whiplash associated disorders [5].

For medium severity pulse according to the EuroNCAP whiplash testing, using the 35% strain injury threshold, the developed FE model predicted an increased risk of injuries to CL for TL, HF and HF/TL seated positions. The highest risk of CL injury for upper and lower cervical spine is for HF and HF/TL seated positions, respectively. This shows that occupants with kyphotic posture are more likely to have CL injured and associated whiplash disorders during the rear end accidents. Similar findings were published in [21], where occupants with kyphotic posture have 70% increased CL elongation than the one with normal lordotic posture.

For ALL, PLL and FL the developed model predicted relatively low peak strains that are below sub-catastrophic failures according to the biomechanical testing.

Table 4. Failure strain in ALL, PLL and LF [25]

	ALL	PLL	LF
Failure strain	80 ± 29%	77 ± 30%	100 ± 43%

S-curvature of the cervical spine occurs during the hypertranslation of the head. The torso and shoulders are pushed forward by the back of the seat, while the head remains stationary. This may lead to protrusion or inward buckling of the ligament flavum (LF) and the increased hydrodynamic pressure in the spinal canal hence injuring the nerve root and causing the head and neck pain [30].

Other than the injury mechanism described, there is currently no published literature that can correlate the level of S-curvature of cervical vertebrae with the nerve root injury threshold. Similar findings were reported by various experimental investigators with PMHS, volunteers isolated cervical spine body segment and numerical models of cervical spine [9], [17], [18], [30]. Therefore, the obtained results can only be used to assess the influence of different seated positions on the level of S-curvature of the neck during the rear end accidents. Clinical findings further support the results that the out of normal seated position can increase the whiplash kinematic and injury. It was noticed that an occupant with kyphosis spine curvature, with no other degenerative change prior to the accident, experienced significantly higher IVD degeneration compared to occupants with normal spine curvature [6].

As with any model of human body, a number of limitations exist that may affect its biofidelity. Soft tissue response is usually obtained at strain rates that are lower than anticipated in traffic accidents. Further simplification of the model such as the exclusion of digestive tract, airways, skin, fat and muscle activation level under constant gravity filed can influence the structural integrity as well as the dynamic response (damping) of the model. Large variation in soft tissue properties as well as published injury threshold [24] presents a major obstacle in implementing FE model of human neck for predicting the injuries to the occupant's soft tissue during the traffic accidents.

5. Conclusion

A detailed and validated FE model cervical spine was used to evaluate the influence of four different occupant seated positions on possible pain sources of whiplash injuries. The model predicted the highest CL strain in the upper cervical spine during the HF seated position, while for the lower portion of the cervical spine the model predicted HF/TL seated position to be most vulnerable. The level of S-curvature of the neck was also evaluated by the model. Although the injury threshold for the nerve root injury has not yet been determined in practice, the model clearly depicts how different seated positions influence the occurrence of S-shape curvature of cervical vertebrae.

The limitations of this study included the lack of the variation of soft tissue mechanical properties for various cervical spine segments. Also the model only depict the behaviour of the 50th percentile male for various occupant seated positions. This makes the model developed a useful tool for assessing the response of general population in rear end accidents.

Future work will include validation tests with volunteers for rear and front impact with measured muscle activations. Additionally, in FE model active Hill-muscle model will be used to evaluate the muscle activation on neck kinematic during the accidents. Individual ligament fibre injuries will also be included using the failure criterion in BEAM finite element for additional assessment of potential whiplash injury.

Beside the presented limitation of the current model, vehicle and road safety designer and engineers can by using it improve their understanding of occupant injury mechanism and further increase the occupant's safety.

Acknowledgment

This study was supported by the Slovenian Research Agency https://www.arrs.gov.si and Austrian Science Fund. https://www.fwf.ac.at.

References

[1] BARNSLEY L., LORD S., BOGDUK N., *Whiplash injury*, Pain, 1994, 58(3), 283–307.

[2] BERTEL RUNE KAALE J.K., ALBREKTSEN G., WESTER K., *Head Position and Impact Direction in Whiplash Injuries: Associations with MRI-Verified Lesions of Ligaments and Membranes in the Upper Cervical Spine*, Journal of Neurotrauma, 2005, 22(11), 8.

[3] CHANG T.K., HSU C.C., CHEN K.T., *Optimal screw orientation for the fixation of cervical degenerative disc disease using nonlinear C3-T2 multi-level spinal models and neuro-genetic algorithms*, Acta Bioeng. Biomech., 2015, 17(3), 59–66.

[4] FICE J., CRONIN D., PANZER M., *Cervical Spine Model to Predict Capsular Ligament Response in Rear Impact*, Annals of Biomedical Engineering, 2011, 39(8), 2152–2162.

[5] FICE J.B., CRONIN D.S., *Investigation of whiplash injuries in the upper cervical spine using a detailed neck model*, J. Biomech., 2012, 45(6), 1098–1102.

[6] HOHL M., *Soft-tissue injuries of the neck in automobile accidents. Factors influencing prognosis*, J. Bone Joint Surg. Am., 1974, 56(8), 1675–1682.

[7] HORST M.J.V.D., *Human Head Neck Response in Frontal, Lateral and Rear End Impact Loading – modelling and validation*, Eindhoven University of Technology, 2002.

[8] JANITZEK T., *Reining in Whiplash Better Protection for Europe's Car Occupants*, European Transport Safety Council ETSC, 2007.

[9] KANEOKA K., ONO K., INAMI S., HAYASHI K., *Motion analysis of cervical vertebrae during whiplash loading.* Spine (Phila Pa 1976), 1999, 24(8), 763–769; discussion 770.

[10] KANG Y.-S., MOORHOUSE K., ICKE K., HERRIOTT R., J.B. IV, *Head and Cervical Spine Responses of Post Mortem Human Subjects in Moderate Speed Rear Impacts*, [in:] IRCOBI Conference 2014, IRCOBI Secretariat – c/o AGU Zurich, 2014.

[11] KEIFER O.P., LAYSON P.D., RECKAMP B.C., *The Effects of Seated Position on Occupant Kinematics in Low-speed Rear-end Impacts*, SAE Technical Paper, 2005-01-1204, 2005.

[12] MICHIEL VAN RATINGEN J.E., AVERY M., GLOYNS P., SANDNER V., VERSMISSEN T., *The Euro NCAP Whiplash Test*, E. NCAP, Editor. 2009.

[13] BOSTROM O.M.Y.S., ALDMAN B., HANSSON H.A., HALAND Y., LOVSUND P., SEEMAN T., SUNESON A., SALJO A., ORTENGREN T., *A new neck injury criterion candidate – Based on injury findings in the cervical spinal ganglia after experimental neck trauma*, [in:] International IRCOBY Conference, Dublin, Ireland, 1996.

[14] PANJABI M., DVORAK J., CRISCO J.J. 3rd, ODA T., WANG P., GROB D., *Effects of alar ligament transection on upper cervical spine rotation*, J. Orthop. Res., 1991, 9(4), 584–593.

[15] PANJABI M.M., ITO S., PEARSON A.M., IVANCIC P.C., *Injury mechanisms of the cervical intervertebral disc during simulated whiplash*, Spine (Phila Pa 1976), 2004, 29(11), 1217–1225.

[16] PEARSON A.M., IVANCIC P.C., ITO S., PANJABI M.M., *Facet joint kinematics and injury mechanisms during simulated whiplash*, Spine (Phila Pa 1976), 2004, 29(4), 390–397.

[17] PENNING L., *Acceleration injury of the cervical spine by hypertranslation of the head*, European Spine Journal, 1992, 1(1), 13–19.

[18] SIEGMUND G.P., MYERS B.S., DAVIS M.B., BOHNET H.F., WINKELSTEIN B.A., *Mechanical evidence of cervical facet capsule injury during whiplash: a cadaveric study using combined shear, compression, and extension loading*, Spine, Phila, Pa 1976), 2001, 26(19), 2095–2101.

[19] SIEGMUND G.P., WINKELSTEIN B.A., IVANCIC P.C., SVENSSON M.Y., VASAVADA A., *The anatomy and biomechanics of acute and chronic whiplash injury*, Traffic Inj. Prev., 2009, 10(2), 101–112.

[20] SPITZER W.O., CASSIDY J.D., D. QUEBEC TASK FORCE ON WHIPLASH-ASSOCIATED, *Scientific Monograph of the Quebec Task Force on Whiplash-Associated Disorders: redefining "whiplash" and its management*, Philadelphia, PA: J.B. Lippincott Co., 1995.

[21] STEMPER B.D., YOGANANDAN N., PINTAR F.A., *Effects of abnormal posture on capsular ligament elongations in a computational model subjected to whiplash loading*, J. Biomech., 2005, 38(6), 1313–1323.

[22] STEMPER B.D., YOGANANDAN N., RAO R.D., PINTAR F.A., *Influence of thoracic ramping on whiplash kinematics*, Clin. Biomech.. Bristol, Avon, 2005, 20(10), 1019–1028.

[23] TEO E.C., ZHANG Q.H., HUANG R.C., *Finite element analysis of head-neck kinematics during motor vehicle accidents: analysis in multiple planes*, Med. Eng. Phys., 2007, 29(1), 54–60.

[24] TRAJKOVSKI A., OMEROVIC S., HRIBERNIK M., PREBIL I., *Failure properties and damage of cervical spine ligaments, experiments and modeling*, J. Biomech. Eng., 2014, 136(3), 031002.

[25] TRAJKOVSKI A., OMEROVIC S., KRASNA S., PREBIL I., *Loading rate effect on mechanical properties of cervical spine ligaments*, Acta Bioeng. Biomech., 2014, 16(3), 13–20.

[26] WALKER L.B., HARRIS E.H., PONTIUS U.R., LA T.U.N.O., *Mass, Volume, Center of Mass and Mass Moment of Inertia of Head and Head and Neck of the Human Body*, Defense Technical Information Center, 1973.

[27] YANG K., ZHU F., LUAN F., ZHAO L., *Development of a Finite Element Model of the Human Neck*, SAE Technical Paper, 1998.

[28] YOGANANDAN N., KUMARESAN S., PINTAR F.A., *Geometric and mechanical properties of human cervical spine ligaments*, J. Biomech. Eng., 2000, 122(6), 623–629.

[29] YOGANANDAN N., PINTAR F.A., ZHANG J., BAISDEN J.L., *Physical properties of the human head: mass, center of gravity and moment of inertia*, J. Biomech., 2009, 42(9), 1177–92.

[30] YOGANANDAN N., STEMPER B.D., RAO R.D., *Patient Mechanisms of Injury in Whiplash-Associated Disorders*, Seminars in Spine Surgery, 2013, 25(1), 67–74.